DOI https: //doi. org/10.1007/s11595-022-2658-0

Early-age Hydration Characteristics of Composite Binder Containing Graphite Powder

HE Wei[1], SONG Shaomin[1*], MENG Xia[2], ZHANG Pengchong[1], SUN Xu[1]

(1. School of Civil and Transportation Engineering, Beijing University of Civil Engineering and Architecture, Beijing 100044, China; 2. Architectural Design and Research Institute of Tsinghua University Co., Ltd., Beijing 100084, China)

Abstract: The early-age hydration characteristics of composite binder containing graphite powder (GP) with two different finenesses were investigated by determining the hydration heat, thermo gravimetric, morphology of hardened paste as well as the compressive strength of mortar. The experimental results show that: replacing 2%-6% of cement with graphite powder significantly improves the piezoresistive effect of early age mortar, can be used to monitor accidental loads caused by dropped objects, collisions, or other accident events, and thus avoids initial damage. Some GP provides additional nucleation sites that lead to a fast formation of hydration products (nucleation-site effect). However, due to the almost hydrophobic water contact angle, most of the GP causes a large number of micro-cracks in the hydrated paste (gap effect). Because of the lamellar shape and high surface energy, GP is easily balled and can not be uniformly distributed in the composite, resulting in clumping together and wrapping some of the cement particles (barrier effect). Due to nucleation-site effect, when the dosages of coarse and fine GP reached 2% and 4%, 1 d strength were increased by 9.1% and 9.6%, respectively. At 3 days, as the interior damage caused by the gap effect gradually increased, and the retarding effect on cement hydration caused by barrier effect was enhanced. GP has an obvious negative effect on compressive strength. However, micro-cracks caused by fine GP are less, so its negative effect on 3 d compressive strength is lower.

Key words: graphite powder; Portland cement; early-age hydration; piezoresistive effect; comprehensive strength

1 Introduction

Concrete has been used as a primary construction material for many years owing to its excellent engineering properties and durability[1]. Although the resistivity of the pore solution in cement paste is only 0.25-0.35 Ω·m[2], the resistivity of the main components of concrete such as aggregates, hydrates and unhydrated cement, are at least tens of thousands of times higher[3,4]. Thus, the resistivity of conventional concrete is usually higher than 10^6 Ω·m[5]. Conventional concrete is a poor electrical conductor, especially under dry conditions.

Electrically conductive concrete (ECC) is a kind of concrete which prepared by adding electrically conductive fillers. After adding, the electric resistivity of concrete can be reduced to a certain value for various applications, such as: resistance heating material for snow and ice melting[6,7], electromagnetic radiation blocker for EMI shielding[8,9], grounding electrode for electric equipment[10,11], self-sensing construction material for traffic motion[12] and structural health monitoring[13,14], electrode material for cathodic protection[15,16], *etc.*

The electrical conductivity of ECC mainly relies on the conductive network formed by conductive fillers to achieve. Under voltage, the current conduction is formed through electrons or holes moving in local conductive net and jumping barrier between electric materials by tunneling effect. When the conductive fillers are not enough to form a conductive network, the resistivity of the concrete reduces slowly with increasing content of conductive fillers. But as soon as the content of conductive fillers reaches to the threshold value, as a

(Received: Sept. 10, 2021; Accepted: Jan. 10, 2022)

HE Wei(何伟): Assoc. Prof.; Ph D; E-mail: hewei@bucea.edu.cn

*Corresponding author: SONG Shaomin(宋少民): Prof.; E-mail: songshaomin@bucea.edu.cn

Funded by the National Natural Science Foundation of China (Nos. 52208413 and 51908022) and the R&D Program of Beijing Municipal Education Commission (Nos. KM202210016011 and KM202110016013)

consequence of the first appearance of the network, the resistivity will show a sudden reduce[17,18].

The conductive fillers used in ECC generally include graphite powder, carbon black, carbon fiber, steel fiber and metal powder, *etc*. The early electrical conductivity of ECC can be well improved by steel fiber and metal powder, but due to the strong alkaline environment of concrete, a non-conductive passivation layer gradually forms, and the conductivity decreases rapidly[19,20]. As an ideal conductive filler, carbon fiber not only improve the conductivity[21,22], but also the mechanical performance of ECC[23]. However, high cost leads to limit its application in engineering. Although the price is low, carbon black needs a very big dosage to present a good performance in reducing electrical resistivity, and it will have a significant negative effect on the workability and strength of concrete[24,25]. Graphite powder is a little more expensive than carbon black, and has the same problems with carbon black, but to a lesser extent than it does[26].Recent research also suggests that when graphite powder and carbon fiber are used together, conductive network can be formed at a relatively low dosage[27]. For one thing, the cost is relatively acceptable, and for another, the negative effect on mechanical performance is acceptable. When a low dosage of graphite powder is used alone, although the graphite-cement based composites still shows a high level of electrical resistivity, the high sensitive linear piezoresistive response demonstrates its potential for application in important structure as a self-sensing material[28].

However, existing research about the effect of graphite powder finenesses and content on the piezoresistive performance of cement-based material is still rare at present. Additionally, as well known, it is evident that the hydration properties of Portland cement are affected by inert powder materials. For example, limestone powder can act as fine filler[29], and its surface can provide additional nucleation sites for the hydration products of cement clinker, which contribute to the development of early strength[30,31]. But so far, there is very little research regarding the influence of graphite powder on the hydration properties of cement, especially in the early age.

In this paper, two flake graphite powder with different finenesses were used as substitutes in the blends. The influence of graphite powder's fineness and dosage on the early-age hydration properties of composite the binder, as well as mortar strength and piezoresistive effect, were investigated.

2 Experimental

2.1 Raw materials

A reference cement in accordance with the Chinese National Standards GB 8076-2008 from China United Cement Corporation was used in this study. The strength grade of the cement is 42.5, and its specific surface area is 312 m^2/kg. The chemical compositions of cement determined by XRF is given in Table 1.

Table 1 Chemical composition of cement/wt%

CaO	SiO_2	Al_2O_3	SO_3	Fe_2O_3	MgO	others
61.48	21.47	4.49	4.12	3.71	3.38	1.35

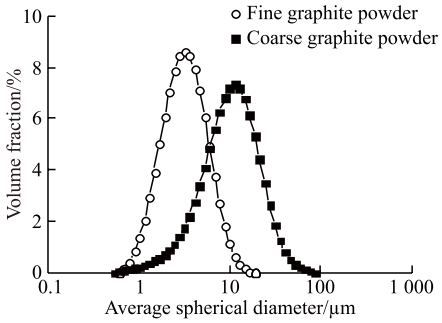

Fig.1 Particle size distribution of graphite powder

High purity graphite powder with two different finenesses were used. The particle size distributions of the graphite powder measured by a laser particle size analyzer (Mastersizer 2000) are presented in Fig.1. It shows that the particle size of the fine graphite powder is significantly smaller than the coarse one. Almost all of the fine graphite powder is smaller than 11 μm. But for the coarse graphite powder, nearly half of it is greater than 11 μm. The specific surface area of the coarse and fine graphite powder are 375.1 and 1 002.0 m^2/kg, respectively.

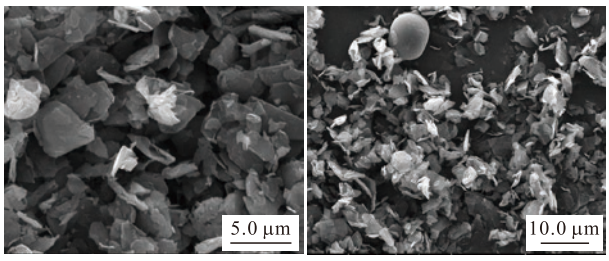

(a) Coarse graphite powder (b) Fine graphite powder

Fig.2 SEM images of graphite powder

SEM images of the coarse and fine graphite powder are shown in Fig.2. It can be seen that the appearance of the coarse and fine graphite powder is almost the same and their shapes are both lamellar.

ISO standard sand complying with the Chinese

National Standard GB/T 17671-1999 was used as fine aggregate. Commercially available powdery naphthalene superplasticizer was used to offset the adverse effects of graphite powder on mortar workability.

2.2 Preparation of samples

In order to reveal the influence of graphite powder with different finenesses on the compressive strength and piezoresistive effect of mortar at an early age, mortar specimens were prepared by mixing reference cement, graphite powder, ISO standard sand, water, and powdery naphthalene superplasticizer.

Due to the significant negative effect on workability and strength[32], graphite powder is often used in conjunction with carbon fiber as conductive filler, at a low dosage, such as 2.5%[33], 10%[34] (mass fraction of cement). What's more, Gan *et al*[28] found that when 3% graphite powder was used alone, although there was little change in mortar electrical resistivity, the piezoresistive effect was significantly enhanced. Thus, in this research, cement was partially replaced by graphite powder residue as 2%, 4%, and 6%.

Table 2 Mix proportions of mortars/wt%

Mortar samples	Composition of the binder			Naphthalene superplasticizer
	Cement	Coarse GP	Fine GP	
MR0	100.00	/	/	0.00
MC2	98.00	2.00	/	0.30
MC4	96.00	4.00	/	0.60
MC6	94.00	6.00	/	0.90
MF2	98.00	/	2.00	0.30
MF4	96.00	/	4.00	0.60
MF6	94.00	/	6.00	0.90

For mortar specimens, the mixing amount of the powdery naphthalene superplasticizer is 0, 0.3%, 0.6%, and 0.9% of the binder, as shown in Table 2. The binder-to-fine aggregate and water-to-binder ratio adopted in this study are 1:3 and 0.5, respectively.

Constituents were weighed separately and then in the laboratory, and then mixed in an electric mortar mixer to ensure homogeneity. Within 24 h, the mortar specimens sized 40 mm×40 mm×160 mm for compressive strength test were demoulded and then were cured in a room with a temperature of 20±1 ℃ and a relative humidity higher than 95% till testing ages (1 and 3 days).

Owing to the advantages of rapid testing, repeatability, and simple geometry factor[35], electrode probe method was adopted to study the piezoresistive responses of the mortar with different content of graphite powder. Copper mesh electrodes were embedded in fresh mortar (as shown in Fig.3), then the specimens were cured at 20±1 ℃ and ⩾95% RH in a standard curing box for 24 h. After 24 h, specimens were removed from the molds and cured until the testing age of 3 days.

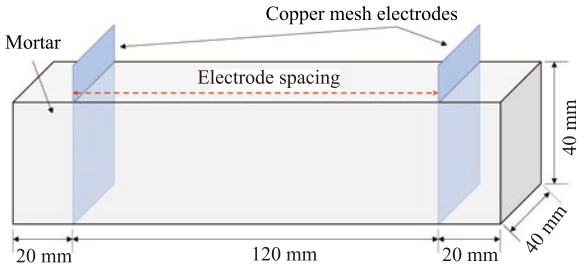

Fig.3 Schematic of specimens with embedded electrode

In order to reveal the influence of graphite powder on the hydration properties of the graphite-cement composite binder, pastes samples were prepared. By removal of sand and naphthalene superplasticizer components, mortar samples were made into pastes. Table 3 shows the mix proportions of the pastes.

Table 3 Mix proportions of pastes/wt%

Paste samples	Composition of the binder		
	Cement	Coarse GP	Fine GP
PR0	100.00	/	/
PC2	98.00	2.00	/
PC4	96.00	4.00	/
PC6	94.00	6.00	/
PF2	98.00	/	2.00
PF4	96.00	/	4.00
PF6	94.00	/	6.00

The paste samples for SEM and BSE tests were mixed uniformly by a mechanical mixer for 3 min and then cast into plastic centrifuge tubes. After that, the tubes were sealed and then were cured in a room with a temperature of 20±1 ℃ till 3 days.

2.3 Test methods

2.3.1 Piezoresistive effect

To avoid measurement difficulty associated with polarization effect induced by direct current (DC) method[36], alternating current (AC) with a frequency of 1000 Hz and sine-wave amplitude of 2.5 V (virtual values 1.7678 V) was generated by a UTG2122B waveform signal generator. The voltage and current values are continuously measured while compressive loading is applied along the length of the specimen using a hydraulic mechanical testing system, as shown in Fig.4.

The bulk resistivity ρ can be calculated according to Eq.(1):

$$\rho = \frac{U}{A} \cdot \frac{S}{L} \tag{1}$$

where, ρ stands for the bulk resistivity, S the cross-sectional area between the electrodes, U the applied voltage, I the current, and L the electrode spacing length.

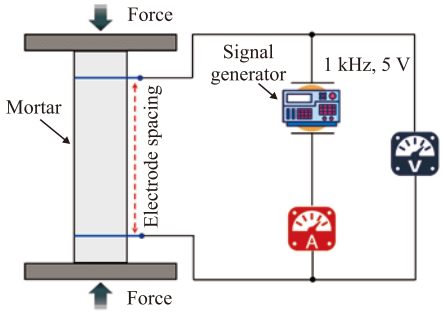

Fig.4 Resistance measurement

2.3.2 Compressive strength

At the age of 1 and 3 days, the compressive strength test was performed for three mortar specimens of each composition, these tests were run in the equipment ShiDai-ShiJin model YE-200A at a loading rate of 2 400 N/s as per Chinese National Standard GB/T 17671-1999. The results were presented as the average of six replicate.

2.3.3 Hydration heat

The hydration heat evolution and total hydration heat of the mixture (cement, graphite powder, and water) were measured using TAM Air Calorimeter with an accuracy of 20 μW at constant temperatures of 25 ℃ within 72 hours. TAM Air Calorimeter has eight parallel twin-chamber measuring channels maintained at a constant temperature: one chamber containing the sample, another containing the reference. After mixing homogeneously, the samples were immediately placed into the chamber. The hydration heat evolution rate of the composite binder can be continuously monitored as a function of time.

2.3.4 SEM, BSE, and TG analyses

At the age of 3 days, the hardened pastes were cut into pieces and put into anhydrous alcohol. The unreacted water in the hardened paste could be removed by anhydrous alcohol due to concentration difference, so the further hydration of cement was stopped. Then, the paste samples were dried overnight in a forced-air oven at 40 ℃. After that, scanning electron microscope (SEM) and back-scattered electron (BSE) tests were performed on PC4 sample, and thermal gravimetric (TG) was performed on all paste samples.

SEM and BSE tests were carried out with QUANTA 200F field emission scanning electron microscope. TG was carried out with a TA Instruments TGA Q5000 V3.17 build 265 under nitrogen at a heating rate of 10 ℃/min from 25 to 900 ℃ in 50.0 mL/min N_2 flow.

3 Results and discussion

3.1 Influence of graphite powder on the early piezoresistive effect of mortars

At the age of 3 days, when no external force is applied, the bulk resistivity (ρ) of MR0 is 23.42 Ω·m. Replacing 2%, 4%, and 6% of the cement with coarse GP cause the bulk resistivity of mortar specimen to reduce to 21.71, 19.17, and 17.71 Ω·m, while using fine graphite powder reduce to 18.94, 17.10, and 16.97 Ω·m. Although increase in graphite powder content or fineness can play a role in enhancing the electric conductivity, the role is not significant. This is partly because the bulk resistivity of early age mortar is low, and partly because the dosage is a little far form percolation threshold value, only beyond which the electrical resistivity is reduced sharply[37].

When ECC is used as self-sensing material for monitoring, it is subjected to external loads, and should be regarded as part of the bearing structure. Thus, in practical application, the data form monitoring is the change of stress, not the value of load. Therefore, at first, the specimen was loaded to 5 MPa at a very slow speed. Then, mechanical compressive stress up to 15 MPa with a loading rate of 0.04 MPa/s was applied to the preloaded specimen. The influence of loading stress on the resistance of mortar with different content of graphite powder are shown in Fig.5. In this figure, the resistance ratio ρ_x/ρ_5 is defined as the ratio of the resistance (ρ_x) of the specimen at x MPa to the resistance of the specimen at 5 MPa.

As can be seen in Fig.5, for MR0, the resistance ratio ρ_x/ρ_5 is lightly inversely related to stress, just decreased by 6.98% when the stress raises from about 5 MPa to 15 MPa, and the linear correlation coefficient barely reaches 0.8963. With the increase of graphite powder content, the reduction rate of ρ_x/ρ_5 and the degree of linearity between ρ_x/ρ_5 and stress are significantly improved. After 6% of the cement was replaced by coarse and fine graphite powder, the resistance ratio is reduced by 31.9% and 29.6%, respectively, and causing correlation coefficient to increase to over 0.99. Additionally, it is obvious that the piezoresistive effect of

coarse graphite powder is higher than fine one for the same dosage (up to 12.1%, 19.7%, and 20.4% at 2%, 4%, and 6%).

As well-known, the increased curing time reduces resistivity due to the hydration progress, which is opposite to the trend of piezoresistive effect. Thus, low dosage of graphite powder (2%-6%, especially efficient at 6%) can well monitor the early-age loads of cement-based material, to avoid initial damages caused by overlarge early loading.

3.2 Influence of graphite powder on the properties of composite binder

3.2.1 Distribution of graphite powder

For the samples with smooth surface, the contrast of BSE image is only related to the atomic number of the sample surface, and has nothing to do with the contrast of the morphology. If there is an uneven distribution of elements on the surface of the sample, the area with a larger average atomic number shows a brighter contrast, otherwise it is displayed as a dark area[38]. The image characteristics (SEM and BSE) of PC4 at the age of 3 days are shown in Fig.6. The dark parts shown in Figs.6(b), 6(d), 6(f), and 6(h) are graphite powder.

As shown in Figs.6(a)-6(b), the surface of graphite powder at AREA 1 is thicker and rougher in SEM image, but thinner and flatter in BSE image, which indicates that the surface of the graphite powder provides additional nucleation sites for the formation of hydration products (named as 'nucleation-site effect'). However, the proportion of this kind of graphite powder is not very high.

To the contrary, Figs.6(c)-6(d) and 6(e)-6(f) show that, for AREA 2 and 3, the appearance of graphite powder in the BSE and SEM images is almost the same, indicating that there is no hydration product covering on, and it will not promote the hydration process. In addition, graphite powder at AREA 2 and 3 have smooth surfaces and lots of gaps with the hydration products. Those micro-defects may cause a decrease in strength (named as 'gap effect').

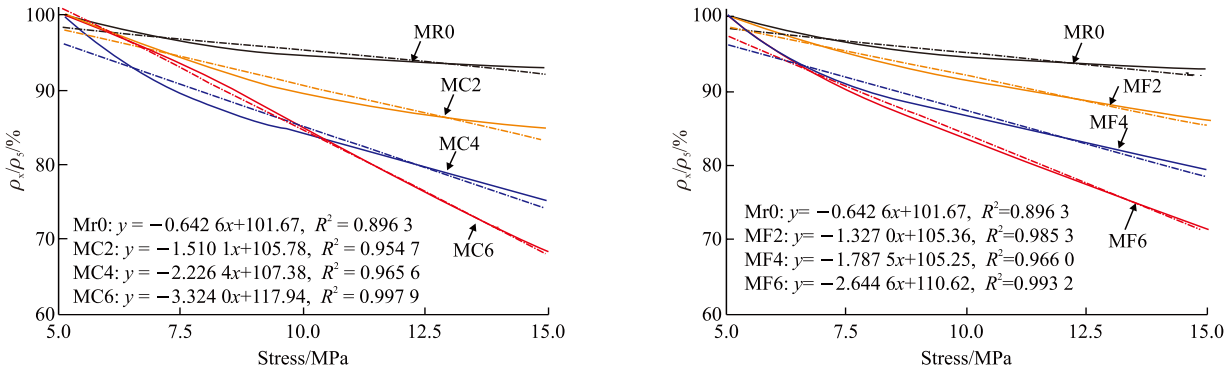

(a) Coarse graphite powder (b) Fine graphite powder

Fig.5 Influence of graphite powder on the piezoresistive effect

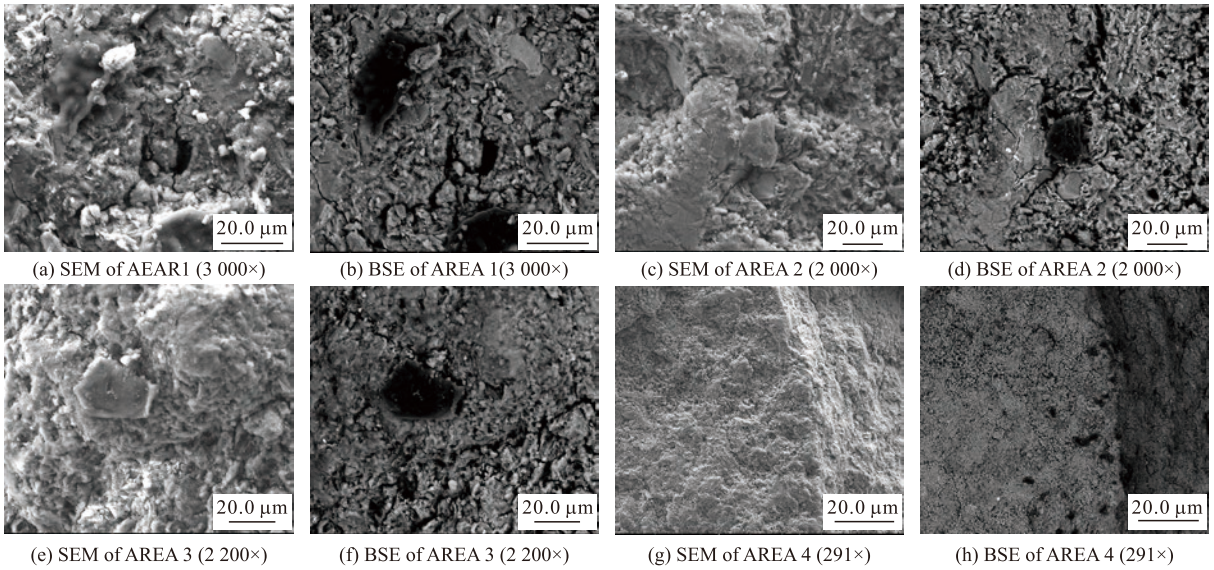

(a) SEM of AEAR1 (3 000×) (b) BSE of AREA 1(3 000×) (c) SEM of AREA 2 (2 000×) (d) BSE of AREA 2 (2 000×)

(e) SEM of AREA 3 (2 200×) (f) BSE of AREA 3 (2 200×) (g) SEM of AREA 4 (291×) (h) BSE of AREA 4 (291×)

Fig.6 SEM and BSE images of PC4 at the age of 3 days

The reason for the contradiction phenomenon between AREA 1 and AREA 2,3 is that graphitic surfaces are nearly hydrophobic with water contact angle within the 75°-98.3° range[39-43]. Generally, when the water contact angle is smaller than 90°, the solid surface is considered hydrophilic and when it is larger than 90°, the solid surface is considered hydrophobic[44]. Since graphite is nearly hydrophobic, only a small number of graphite powder surfaces have hydration products, and most surfaces have no hydration products.

After the magnification is reduced by nearly 10 times, it is seen from Figs.6(g)-6(h) that due to the high surface energy (54.8 mJ/m^2 at room temperature)[45], graphite powder has bad dispersion and obvious aggregate phenomenon[46], resulting in graphite powder clumping together and wrapping some cement particles (named as 'barrier effect'). On the one hand, the barrier effect reduces the contact between water and cement particles to some extent, resulting in retarding the dissolution of the cement particles (as shown Fig.7(a)). On the other hand, the ions diffusion of the wrapped cement particles was also delayed by the barrier effect. Due to the high ions content surrounding cement particles, the further hydration of the cement particles was retarded (as shown Fig.7(b)).

3.2.2 Hydration heat

The influence of graphite powder on the exothermal rate of the graphite-cement composite binders are shown in Fig.8.

As shown in Fig.8, due to the barrier effect, the induction periods of all the samples containing graphite powder were extended. Because of the nucleation-site effect, the induction period was extended, and the dissolution at the beginning of the acceleration period was improved. Thereby, after adding 4%, 6% of coarse graphite powder and 2%, 4%, 6% of fine graphite powder, the second hydration exothermal peak was increased from 3.92 mW/g to 4.14, 4.08, and 4.01, 4.12, and 4.12 mW/g. However, for 2% coarse graphite powder replacement level, the total surface area of graphite powder is smaller than any other sample, having lowest effect on providing additional nucleation sites. Thus, when 2% cement was replaced by coarse graphite powder, the second hydrated exothermic peak was decreases from 3.92 to 3.81 mW/g.

In addition, the occurrence time of the second exothermic peak was also delayed by graphite powder, and the more it was added, the greater the effect. For the control sample (PR0), the occurrence time for the second rate of hydration rate is about 10.11 h after introduction of water. However, after 2%, 4%, 6% of coarse and fine graphite powder added, the appearance time of the second hydration peak is delayed by 9.4%, 20.4%, 26.2%, and 10.1%, 23.8%, 25.1%. It seems like that the effect of coarse and fine graphite powder on the appearance time of the second hydration peak is almost

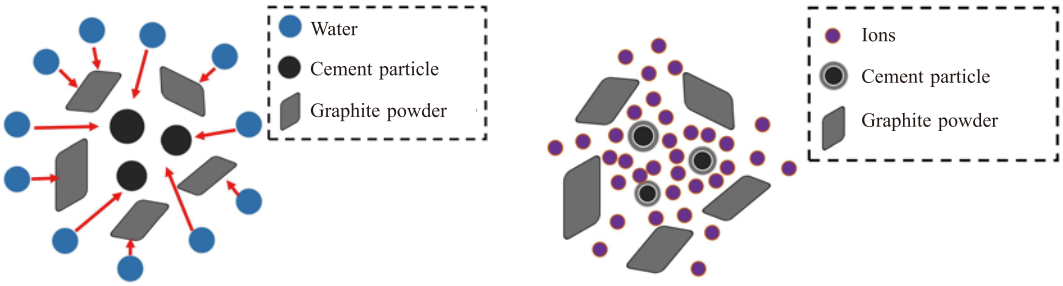

(a) Retarding dissolution (b) Delaying the ions diffusion

Fig.7 Schematic diagram of the barrier effect

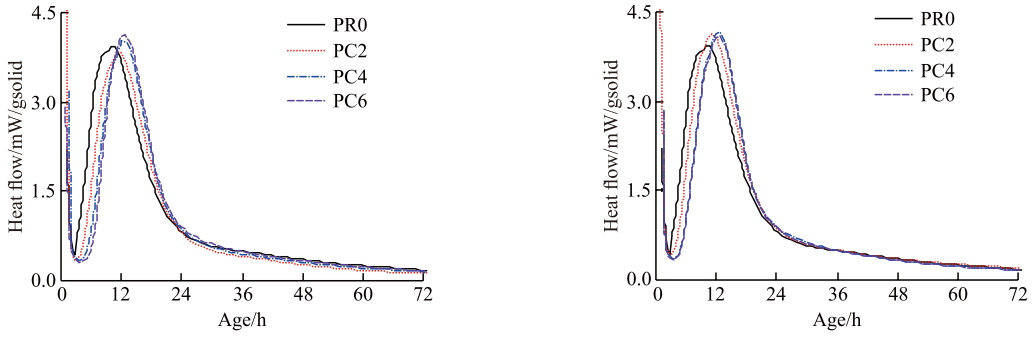

(a) Retarding dissolution (b) Delaying the ions diffusion

Fig.8 Exothermal evolution rate of graphite-cement pastes with increasing replacement level of graphite from 0% to 6% of solids by weight

the same. After 24 h, both coarse and fine graphite powder have no significant influence on the exothermic curve of hydration after 24 h.

3.2.3 Calcium hydroxide content

Calcium hydroxide (CH) is one of the major hydration products of cement. Its decomposition temperature range is different from any other hydration products, such as C-S-H and AFT. Thus, the amount of CH in hardened paste can be determined by thermo gravimetric analysis (TG) and derivative thermo gravimetric (DTG). To a certain extent, its content can be used to represent the hydration degree of the binder.

The decomposition formula of CH is as follows:

$$Ca(OH)_2 \rightarrow CaO + H_2O\uparrow \qquad (2)$$

CH usually decomposes in a temperature interval about from 300 to 500 ℃, and its content can be calculated by the following formula[47]:

$$CH = \frac{M_2}{M_1} m_1 \qquad (3)$$

where, M_1 is the molecular weight of H_2O, M_1=18; M_2 the molecular weight of CH, M_2=74; m_1 the weight losses measured from the TG curves between the initial and final temperatures of the corresponding DTG peaks.

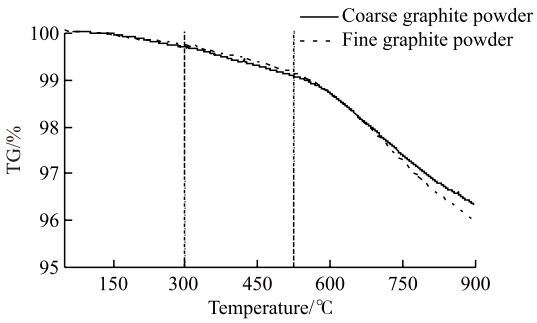

Fig.9 TG curve of the graphite powder

Fig.9 shows characteristic shapes of TG curves of graphite powder with two finenesses. In N_2 gas, the melting point of graphite is at least 4 000 ℃[48], but impurities in graphite ore or grinding aids added during the grinding process are easy to decompose in relatively low temperature. In the temperature range of 300-500 ℃, the mass loss of the coarse and fine graphite powder is almost the same, only 0.5436% and 0.5053%, respectively. However, after the temperature is higher than 600 ℃, the TG curves decrease rapidly.

After being calculated, when the dosage of graphite powder is up to 6%, the mass loss rate of the paste caused by graphite powder in the temperature range of 300-500 ℃ is 0.03262% (for coarse graphite powder) and 0.03032% (for fine graphite powder), which are obviously less than the CH content in the hardened pastes hydrated for 3 days. Thus, the influence of graphite powder decomposition on the analysis of CH content can be ignored.

Fig.10 shows characteristic shapes of TG/DTG curves of the hydrated pastes containing graphite powder with different finenesses after 3 days of curing.

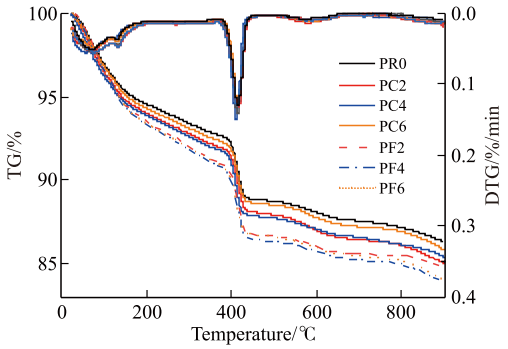

Fig.10 TG/DTG curve of the graphite-cement composite binder hydrated for 3 days

As can be seen from Fig.10, DTG curves are similar in shape, but significant differences can be observed in TG curves, indicating that although graphite powder doesn't modify the composition of the cement hydration products, it caused a significant change in content. The temperature ranges of thermal decomposition of hydration products have great discrepancy in different studies[47,49,50]. The recent research[51] shows that 81-91 ℃ for dehydration of AFt, 80-240 ℃ for major dehydration of C-S-H, 241-244 ℃ for hydrogarnet, 129-138 ℃ for AFm, 411-427 ℃ for $Ca(OH)_2$, and 648-691 ℃ for $CaCO_3$. Since the decomposition temperature range of the main hydration products is less than 427 ℃, and after adding graphite powder, the mass loss up to 427 ℃ is bigger, indicating that graphite powder has a significant promoting effect on the hydration of the composite binder.

According to Formula 2, CH content can be calculated from the mass losses measured from the TG curves between the initial and final temperatures of the corresponding DTG peaks, as shown in Fig.11.

As shown in Fig.11, at the age of 3 days, whether graphite powder is coarse or fine, CH content increases first, and then decreases with the increasing dosage of graphite powder. The reason for this phenomenon is that graphite powder provided additional nucleation sites for CH growth, and with graphite powder content increased, its dispersion decreased, the barrier effect was enhanced, thereby delaying the hydration process.

In addition, similar to fly ash[52] and limestone powder[3], after cement was replaced by graphite powder, the effective water to cement ratio was increased, and the cement hydration was promoted. However, due to the reduction in cement component, after maximum value reaches, with the increasing of content, the CH content gradually decreases.

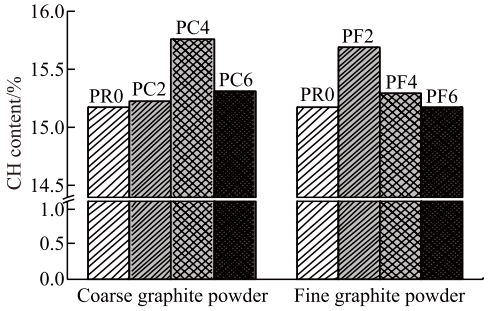

Fig.11 CH content of paste containing graphite powder with different finenesses

It can also be seen in Fig.11 that 2% fine graphite powder increased the CH content by 3.4%. But for coarse graphite powder, its dosage should reach 4% to make the CH content achieve a similar value. This may due to the fact that fine graphite powder has a larger specific surface area, and at the same replacement ratio, it can provide more nucleation sites for the growth of CH.

3.3 Influence of graphite powder on the early compressive strength of mortars

1-d and 3-d compressive strength of the control and graphite powder mortars are shown in Fig.12.

It can be seen from Fig.12(a) that, in general, 1-day compressive strength increases at first and then decreases with coarse or fine graphite powder content. Under a relative low dosage (2%), the enhancing effect of fine graphite powder on mortar strength is not as good as that of coarse graphite powder. However, under a relative high dosage (6%), weakening effect of fine graphite powder on strength is less than that of coarse graphite powder. 1-day compressive strength of the control mortar (MR0) is 17.45 MPa, and it can be increased by 9.1% and 9.6% under the optimum mix amount of coarse and fine graphite powder, respectively. This is probably due to the fact that within the first 24 hours of portland cement hydration, the major hydration products are CH and AFt[53], and graphite powder can increase CH content. In addition, because of the large specific surface area, graphite powder may fill and fine the pores and capillary pores in hardened paste as well.

On the other hand, as shown in Fig.12(b), coarse and fine graphite powder have significant negative impact on 3-day compressive strength. After adding 2%, 4%, and 6% of coarse and fine graphite powder, the 3-d compressive strength was decreased by 13.8%, 17.1%, 19.1%, and 9.4%, 14.0%, and 15.7%. Although graphite powder has a serious adverse effect on the mortar strength, the further deterioration at a relatively large dosage is acceptable. What's more, at the same dosage, the adverse effect of fine graphite on mortar strength is smaller than that of coarse graphite. This phenomenon probably due to the fact that the gaps between fine graphite powder and hardened paste is smaller than the coarse one.

4 Conclusions

a) When graphite powder is used as the only conductive component and the dosage is much lower than percolation threshold, such as 2%-6% of the binder, although the conductivity of the graphite-cement based composites can not be significantly improved, the piezoresistive effect will be significantly enhanced. The results demonstrate the potential usefulness of low dosage of graphite powder as self-sensing construction material. Generally, better piezoresistive effect can be obtained either by increasing graphite powder content or using coarse graphite powder (500 mesh) rather than

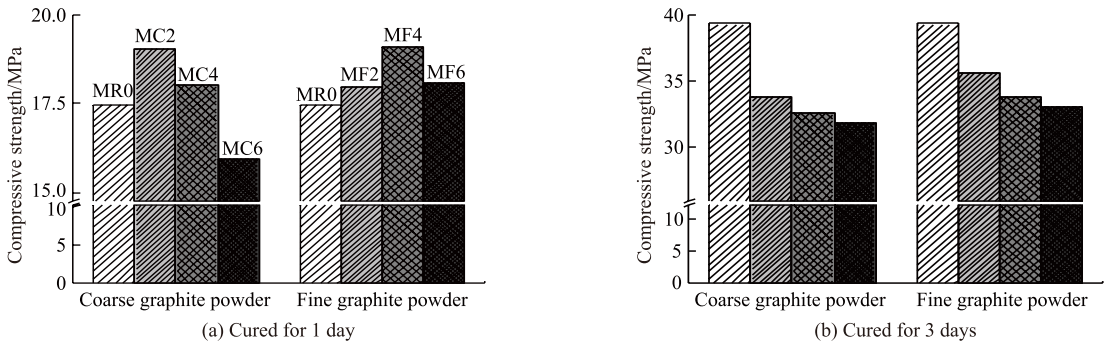

Fig.12 Compressive strength of mortar

fine (5000 mesh).

b) Although it's difficult for graphite powder to form chemical bonds with hydration product or cement, it still has a significant influence on the hardened paste and the hydration process of cement. Shown in the following several aspects: Some of the graphite powder provides additional nucleation sites, resulting in some hydration products growing on it (Nucleation-site effect); However, because of the high water contact angle, most of the graphite powder not only has no hydration product covered with, but also has lots of gaps with the hydration products, causing interior damage to the hardened paste (Gap effect); Because of the lamellar shape and high surface energy, graphite powder easily clump together, and part of the cement particles are usually encapsulated by them (Barrier effect). The barrier effect of graphite powder not only hinders the contact between cement and water, but also blocks the outward diffusion of ions near cement particles.

c) Due to the barrier effect, the induction periods of the samples containing fine or coarse graphite powder are extended. With the increase of induction period, the dissolution degree of the cement particles at the beginning of the acceleration period was higher. In addition, the hydration rate was enhanced by nucleation-site effect. Thus, the second hydration exothermic peak has a maximum increase of 5.1% when the coarse graphite powder content is 4%, 6% and the fine graphite powder content is 2%, 4%, and 6%. However, for the group with 2% coarse graphite powder, the surface area for nucleation sites is smaller. So that when 2% cement was replaced by coarse graphite powder, the hydration exothermic peak is 2.8% lower than the control group.

d) As graphite powder provides additional nucleation sites that lead to a fast formation of hydration products, 1-d compressive strength of the mortar was increased by 9.1% and 9.6% under the optimum mix amount of coarse and fine graphite powder, respectively. However, due to micro-cracks causing by graphite powder, the 3-d compressive strength was significantly decreased. Under the same dosage, the micro-cracks caused by fine graphite powder are smaller, so the adverse effect of fine graphite powder is slightly lower than coarse graphite powder.

References

[1] Shi MX, Wang Q, Zhang ZK. Comparison of the Properties between High-volume Fly Ash Concrete and High-volume Steel Slag Concrete under Temperature Matching Curing Condition[J]. *Construction & Building Materials*, 2015(98): 649-655

[2] McCarter WJ, Forde MC, Whittington HW. Resistivity Characteristics of Concrete[J]. *Proceedings of the Institution of Civil Engineers*, 1981, 71(1): 107-117

[3] WHITING DA, NAGI MA. *Electrical Resistivity of Concrete - A Literature Review*[R]. Illinois: Portland Cement Association, 2003

[4] Monfore GE. The Electrical Resistivity of Concrete[J]. *Journal of the PCA Research & Development Laboratories*,1968, 10(2): 35-48

[5] Han BG, Ou JP, Zhang LQ. *Smart and Multifunctional Concrete toward Sustainable Infrastructures*[M]. Singapore: Springer Nature Singapore PTE Ltd., 2017: 247

[6] Wu JM, Liu JG, Yang F. Three-phase Composite Conductive Concrete for Pavement Deicing[J]. *Construction & Building Materials*, 2015(75): 129-135

[7] Tuan CY. Roca Spur Bridge: The Implementation of an Innovative Deicing Technology[J]. *Journal of Cold Regions Engineering*, 2008, 22(1): 1-15

[8] Dai YW, Sun MQ, Liu CG, *et al*. Electromagnetic Wave Absorbing Characteristics of Carbon Black Cement-based Composites[J]. *Cement & Concrete Composites*, 2010, 32(7): 508-513

[9] Muthusamy S, Chung DDL. Carbon-fiber Cement-based Materials for Electromagnetic Shielding[J]. *ACI Materials Journal*, 2010, 107(6): 602-610

[10] Wang JR, Ding YM. The Application of Conductive Concrete in the Grounding Network Reconstruction of Bai-Sha Hydropower Station[J]. *Electrical Equipment*, 2008, 9(4): 67-69

[11] Zhang J, Xu L, Zhao Q. Investigation of Carbon Fillers Modified Electrically Conductive Concrete as Grounding Electrodes for Transmission Towers: Computational Model and Case Study[J]. *Construction & Building Materials*, 2017(145): 347-353

[12] Shi ZQ, Chung DDL. Carbon Fiber-reinforced Concrete for Traffic Monitoring and Weighing in Motion[J]. *Cement & Concrete Research*, 1999, 29(3): 435-439

[13] Zhang XY, Lü Y, Chen J, *et al*. Field Sensing Characteristic Research of Carbon Fiber Smart Material[J]. *Journal of Wuhan University of Technology-Mater. Sci. Ed*., 2015, 30(5): 914-917

[14] Howser RN, Dhonde HB, Mo YL. Self-sensing of Carbon Nano-fiber Concrete Columns Subjected to Reversed Cyclic Loading[J]. *Smart Materials & Structures*, 2011, 20(8): 085031

[15] Fu XL, Chung DDL. Radio-wave-reflecting Concrete for Lateral Guidance in Automatic Highways[J]. *Cement & Concrete Research*, 1998, 28(6):795-801

[16] Yehia S, Host J. Conductive Concrete for Cathodic Protection of Bridge Decks[J]. *ACI Materials Journal*, 2010, 107(6): 577-585

[17] Xie P, Gu P, Beaudoin JJ. Electrical Percolation Phenomena in Cement Composites Containing Conductive Fibers[J]. *Journal of Materials Science*, 1996, 31(15): 4093-4097

[18] Chen B, Wu K, Yao W. Conductivity of Carbon Fiber Reinforced Cement-based Composites[J]. *Cement & Concrete Composites*, 2004, 26(4): 291-297

[19] Banthia N, Djeridance S, Pigeon M. Electrical Resistivity of Carbon and Steel Micro-fiber Reinforced Cements[J]. *Cement & Concrete Research*, 1992, 22(5): 804-814

[20] Yehia S, Tuan CY, Ferdon D, et al. Conductive Concrete Overlay for Bridge Deck Deicing: Mixture Proportioning, Optimization, and Properties[J]. *ACI Materials Journal*, 2000, 97(2): 172-181

[21] Chung DDL. Self-monitoring Structural Materials[J]. *Materials Science & Engineering R: Reports*, 1998, 22(2): 57-78

[22] Chiarello M, Zinno R. Electrical Conductivity of Self-monitoring CFRC[J]. *Cement & Concrete Composite*, 2005, 27(4): 463-469

[23] Shui ZH, Li C, Liao WD. Resistance Responses of Carbon Fiber Cement to Cycled Compressive Stresses[J]. *Journal of Wuhan University of Technology-Mater. Sci. Ed.*, 2005, 20(4): 116-119

[24] Han BG, Chen W, Ou JP. Piezo Resistivity of Cement-based Materials with Acetylene Carbon Black[J]. *Acta Materiae Compositae Sinica*, 2008, 25(3): 39-44

[25] Wang XY, Sun MQ, Hou ZF, *et al.* Study on Electrical and Electro Thermal Properties of Nano Carbon Black Cement Mortar[J]. *Journal of Functional Materials*, 2006, 37(11): 1841-1843+1847

[26] Yang YS, Dong FQ. On Electro Thermal Concrete of Doping Graphite Electricity-conductive Elementary Materials[J]. *Journal of Functional Materials*, 2008, 39(3): 385-387

[27] Wen S, Chung DDL. Partial Replacement of Carbon Fiber by Carbon Black in Multifunctional Cement-matrix Composites[J]. *Carbon*, 2007, 45(3): 505-513

[28] Gan WM, Huang X, Chen PF. Piezoresistivity of Cement Based Material with Small Amount of Graphite[J]. *Journal of Beijing University of Aeronautics and Astronautics*, 2011, 37(5): 556-559+578

[29] Rahhal V, Bonavetti V, Trusilewicz L, *et al.* Role of the Filler on Portland Cement Hydration at Early Ages[J]. *Construction & Building Materials*, 2012(27): 82-90

[30] Wang YS, Lü LN, He YJ, *et al.* Effect of Calcium Silicate Hydrate Seeds on Hydration and Mechanical Properties of Cement[J]. *Journal of Wuhan University of Technology-Mater. Sci. Ed.*, 2021, 36(1): 103-110

[31] Wang Q, Yang J, Chen HH. Long-term Properties of Concrete Containing Limestone Powder[J]. *Materials & Structures*, 2017, 50(3): 168

[32] Cui SP, Liu YX, Lan MZ, *et al*. Preparation and Properties of Graphite-cement Based Composites[J]. *Journal of the Chinese Ceramic Society*, 2007, 35(1): 91-95

[33] Chen M, Gao P, Geng F, *et al.* Mechanical and Smart Properties of Carbon Fiber and Graphite Conductive Concrete for Internal Damage Monitoring of Structure[J]. *Construction & Building Materials*, 2017(142): 320-327

[34] Cao HY, Yao W, Qin JJ. Seebeck Effect in Graphite-carbon Fiber Cement Based Composite[J]. *Advanced Materials Research*, 2011(177): 566-569

[35] Sassani A, Ceylan H, Kim S, *et al*. Influence of Mix Design Variables on Engineering Properties of Carbon Fiber-modified Electrically Conductive Concrete[J]. *Construction & Building Materials*, 2017(152): 168-181

[36] Chen B, Wu K, Yao W. Conductivity of Carbon Fiber Reinforced Cement-based Composites[J]. *Cement & Concrete Composites*, 2004(26): 291-297

[37] Han BG, Ding SQ, Yu X. Intrinsic Self-sensing Concrete and Structures: A Review[J]. *Measurement*, 2015(59): 110-128

[38] Zhang QQ, Wei Y. Quantitative Analysis on Reaction Degree of Slag-cement Composite System Based on Back-scattered-electron Image[J]. *Journal of the Chinese Ceramic Society*, 2015, 43(5): 563-569

[39] Fowkes FM, Harkins WD. The State of Monolayers Adsorbed at the Interface Solid-Aqueous Solution[J]. *Journal of the American Chemical Society*, 1940, 62(12): 3 377-3 386

[40] Tadros ME, Hu P, Adamson AW. Adsorption and Contact Angle Studies: I. Water on Smooth Carbon, Linear Polyethylene, and Stearic Acid-coated Copper[J]. *Journal of Colloid & Interface Science*, 1974, 49(2): 184-195

[41] Shin YJ, Wang Y, Huang H, *et al*. Surface Energy Engineering of Grapheme[J]. *Langmuir the ACS Journal of Surfaces and Colloids*, 2010, 26(6): 3798-802

[42] Kogan MJ, Dalcol I, Gorostiza P, *et al.* Supramolecular Properties of the Proline-rich γ-Zein N-Terminal domain[J]. *Biophysical Journal*, 2002, 83(2): 1 194-1 204

[43] Raj R, Maroo SC, Wang EN. Wettability of Graphene[J]. *Nano Letters*, 2013, 13(4): 1 509-1 515

[44] Zheng Y, Zaoui A. Wetting and Nanodroplet Contact Angle of the Clay 2:1 Surface: The Case of Na-montmorillonite (001)[J]. *Applied Surface Science*, 2016, 396: 717-722

[45] Wang SR, Zhang Y, Abidi N, Cabrales L. Wettability and Surface Free Energy of Graphene Films[J]. *Langmuir*, 2009, 25(18): 11 078-11 081

[46] Jia XW, Zhang X, Ma D, *et al*. Conductive Properties and Influencing Factors of Electrically Conductive Concrete: A Review[J]. *Materials Review*, 2017(21): 93-100

[47] Dweck J, Buchler PM, Acv C, *et al.* Hydration of a Portland Cement Blended with Calcium Carbonate[J]. *Thermochimica Acta*, 2000, 346(1): 105-113

[48] Savvatimskii AI, Aleksandr I. Melting Point of Graphite and Liquid Carbon[J]. *Physics-Uspekhi*, 2003, 46(12): 1 295-1 303

[49] Wang K, Shah SP, Mishulovich A. Effects of Curing Temperature and NaOH Addition on Hydration and Strength Development of Clinker-free CKD-fly Ash Binders[J]. *Cement & Concrete Research*, 2004, 32(2): 299-309

[50] Vassileva CG, Vassilev SV. Behaviour of Inorganic Matter During Heating of Bulgarian Coals: 1. Lignites[J]. *Fuel Processing Technology*, 2005, 86(12-13): 1 297-1 233

[51] Song H, Jeong Y, Bae S, *et al.* A Study of Thermal Decomposition of Phases in Cementitious Systems Using HT-XRD and TG[J]. *Construction & Building Materials*, 2018(169): 648-661

[52] Wang Q, Wang DQ, Chen HH. The Role of Fly Ash Microsphere in the Microstructure and Macroscopic Properties of High-strength Concrete[J]. *Cement & Concrete Composite*, 2017(83): 125-137

[53] Soroka J. *Portland Cement Paste and Concrete*[M]. London: Macmillan Press Ltd, 1979: 35